Hyperfine Interact (2014) 226:89–97
DOI 10.1007/s10751-013-0966-7

# Mössbauer study of $Cu_{1-x}Zn_xFe_2O_4$ catalytic materials

**K. Koleva · N. Velinov · T. Tsoncheva · I. Mitov**

Published online: 3 December 2013


**Abstract** Copper zinc ferrites ($Cu_{1-x}Zn_xFe_2O_4$) with different composition (x = 1; 0.2; 0.5; 0.8) were prepared by conventional thermal method. Formation of well crystallized ferrite phase with cubic structure and crystallites size of about 19.08–24.39 nm was observed by Powder X-ray diffraction and Mössbauer spectroscopy. The ferrite materials were tested as catalysts in methanol decomposition to CO and $H_2$. A strong dependence of the catalytic behaviour of $Cu_{1-x}Zn_xFe_2O_4$ ferrites of their composition and the phase transformations which occurred under the reaction medium was established.

**Keywords** Nanocrystalline ferrite · Mössbauer spectroscopy · Methanol decomposition

## 1 Introduction

The Mössbauer effect is one of the most interesting phenomena of physics with broad theoretical and practical applications. It depends on the chemical and intermolecular bonds involving the nucleus, which becomes a tool for the study of crystalline and amorphous compounds [1]. $^{57}$Fe Mössbauer spectroscopy studies have been widely used in different field of scientific investigations because it is useful and sensitive technique for analysis of the Fe-bearing phases such as magnetic materials, biological, astrobiology, minerals [2–5]. The hyperfine parameters such as isomer shift, quadruple split, magnetic field provide information about magnetic behavior, cation distribution and oxidation state of iron ions.

The spinel ferrites are denoted with general formula $AB_2O_4$. The distribution of metal ions in crystal lattice determines ferrites as normal, inverse and partial inverse ones. It was

Proceedings of the 32nd International Conference on the Applications of the Mössbauer Effect (ICAME 2013) held in Opatija, Croatia, 1–6 September 2013.

K. Koleva (✉) · N. Velinov · I. Mitov
Institute of Catalysis, BAS, Sofia, 1113, Bulgaria
e-mail: kremena_vassileva@abv.bg

T. Tsoncheva
Institute of Organic Chemistry with Centre of Phytochemistry, BAS, Sofia, 1113, Bulgaria

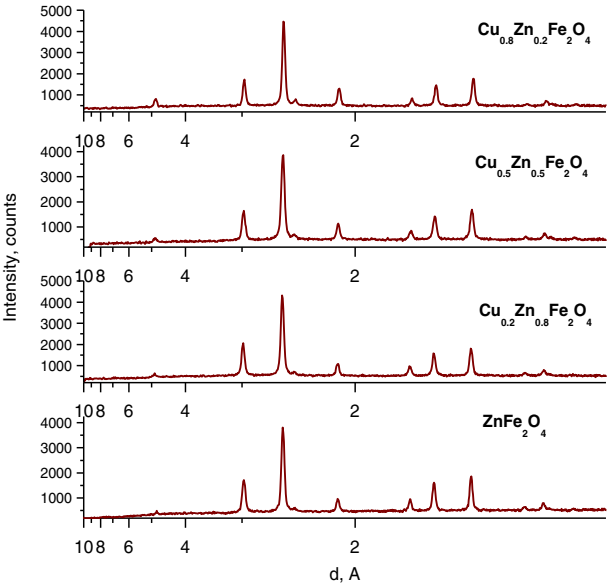


**Fig. 1** X-ray analysis of the investigated samples

established that the position and the oxidative state of the cations influence their structural, magnetic, electrical, catalytic and chemical properties [6–11]. In the $ZnFe_2O_4$ ferrite the tetrahedral (A) sites are occupied by only one type of cations. This is because of the preferences of $Zn^{2+}$ to occupy the tetrahedral spinel sites forming normal spinel, while $Cu^{2+}$ occupies mainly the octahedral [B] sites, and thus, the tetrahedral sites are occupied by half of $Fe^{3+}$ and $CuFe_2O_4$ describes as fully inverse spinel. In the case of $Cu_{1-x}Zn_xFe_2O_4$, where $0 < \times < 1$, the tetrahedral sites are occupied both by $Zn^{2+}$ and $Fe^{3+}$ cations and this spinel structure are denoted as partially inverse.

The aim of present work is to prepare nanocrystalline ferrites with different chemical compositions $Cu_{1-x}Zn_xFe_2O_4$ (x = 0.2, 0.5, 0.8, 1) and to study their catalytic behaviour in methanol decomposition to CO and hydrogen. The cations distribution in ferrites and the phase transformations under the reaction medium were also in the focus of the study.

## 2 Experimental

### 2.1 Synthesis

$Cu_{1-x}Zn_xFe_2O_4$ ferrite materials (x = 0.2, 0.5, 0.8 or 1.0) were prepared by coprecipitation method according to the procedure described in [12]. The solution of $Zn(NO_3)_2.6H_2O$, $Fe(NO_3)_3.9H_2O$ and $Cu(NO_3)_2.3H_2O$ was precipitated with dropwise addition of 1 M $Na_2CO_3$ up to pH = 9 and continuous stirring. The obtained precipitate was washed with distilled water, dried at room temperature and treated at 773 K for 4 hours.

**Table 1** Average crystallites size (D), degree of microstrain (e) and lattice parameters determined from XRD patterns of $Cu_xZn_{1-x}Fe_2O_4$

| Sample | Phase | D, nm | $e \times 10^3$ | a, Å |
|---|---|---|---|---|
| $ZnFe_2O_4$ | Fd3m(227)-cubic | 19.08 | 1.228 | 8.43 |
| $Cu_{0.2}Zn_{0.8}Fe_2O_4$ | Fd3m(227)-cubic | 19.81 | 1.077 | 8.42 |
| $Cu_{0.5}Zn_{0.5}Fe_2O_4$ | Fd3m(227)-cubic | 21.79 | 2.797 | 8.41 |
| $Cu_{0.8}Zn_{0.2}Fe_2O_4$ | Fd3m(227)-cubic | 24.39 | 1.764 | 8.38 |

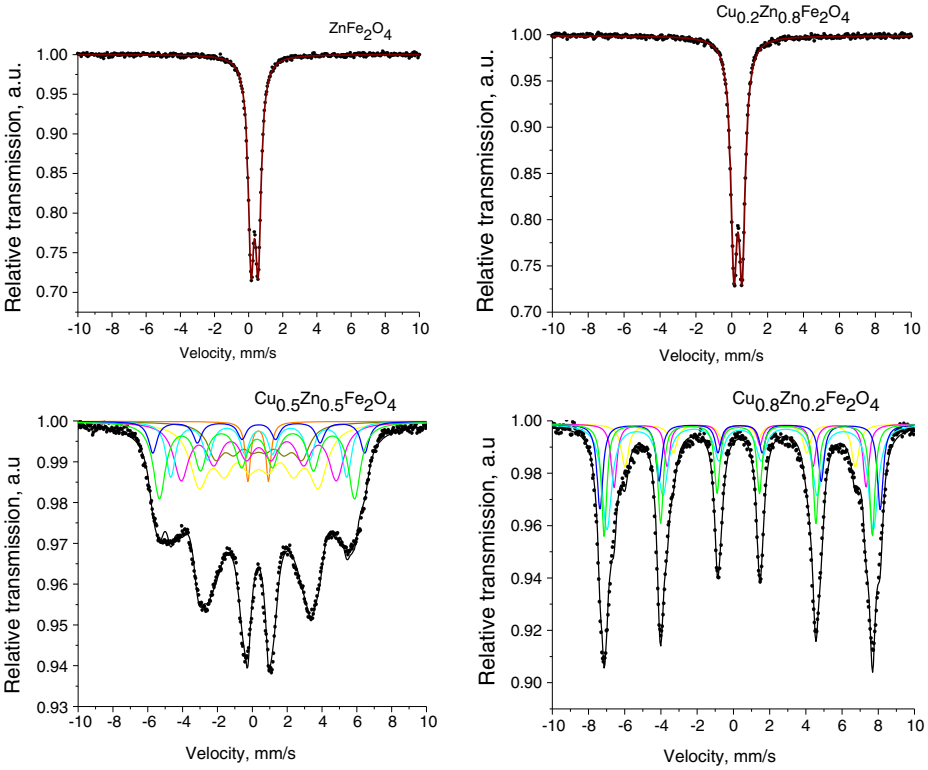


**Fig. 2** Mössbauer spectra of $Cu_{1-x}Zn_xFe_2O_4$

## 2.2 Methods of characterization

The powder X-Ray Diffraction (XRD) patterns were recorded by use of a TUR M62 diffractometer with Co K$\alpha$ radiation. The average crystallites size (D), the degree of microstrain (e) and the lattice parameters (a) of the studied ferrites were determined from the experimental XRD profiles by using the PowderCell−2.4 software [13]. The instrumental broadening of diffraction peaks is equal to 0.020° Bragg angle. It was determined by Al standard and was excluded at calculation of crystallites size and the degree of microstrain. The Mössbauer spectra were obtained at room temperature (RT) and liquid nitrogen temperature (LNT) with a Wissel (Wissenschaftliche Elektronik GmbH, Germany) electromechanical spectrometer

**Table 2** Parameters of Mössbauer spectra of $Cu_xZn_{1-x}Fe_2O_4$

| Sample | Components | $\delta$, mm/s | $\Delta$, mm/s | B, T | $\Gamma_{exp}$, mm/s | G, % |
|---|---|---|---|---|---|---|
| $ZnFe_2O_4$ | Db | 0.35 | 0.42 | – | 0.41 | 100 |
| $Cu_{0.2}Zn_{0.8}Fe_2O_4$ | Db | 0.35 | 0.46 | – | 0.43 | 100 |
| $Cu_{0.5}Zn_{0.5}Fe_2O_4$ | Sx1-tetra, A | 0.27 | 0.46 | 32.0 | 0.91 | 25 |
| | Sx2-octa, B1 (0.09) | 0.37 | 0.00 | 34.6 | 0.75 | 15 |
| | Sx3-octa, B2 (0.23) | 0.37 | 0.00 | 28.5 | 0.77 | 18 |
| | Sx4-octa, B3 (0.31) | 0.37 | 0.00 | 23.7 | 0.60 | 10 |
| | Sx5-octa, B4 (0.23) | 0.37 | 0.00 | 18.7 | 1.02 | 24 |
| | Sx6-octa, B5 (0.09) | 0.37 | 0.00 | 5.6 | 0.75 | 15 |
| | Db | 0.34 | 1.17 | – | 0.35 | 3 |
| $Cu_{0.8}Zn_{0.2}Fe_2O_4$ | Sx1-tetra, A | 0.27 | 0.00 | 46.0 | 0.35 | 25 |
| | Sx2-octa, B0 (0.26) | 0.37 | 0.00 | 48.0 | 0.39 | 17 |
| | Sx3-octa, B1 (0.39) | 0.37 | 0.00 | 45.0 | 0.65 | 34 |
| | Sx4-octa, B2 (0.25) | 0.37 | 0.00 | 43.2 | 0.38 | 12 |
| | Sx5-octa, B3 (0.08) | 0.37 | 0.00 | 39.5 | 0.49 | 10 |

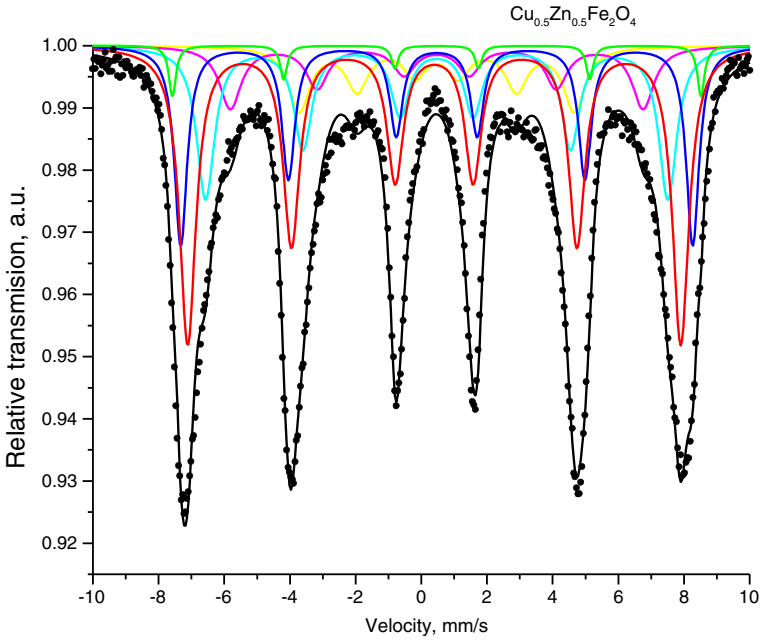


**Fig. 3** Mössbauer spectrum of $Cu_{0.5}Zn_{0.5}Fe_2O_4$ sample at LNT

working in a constant acceleration mode. $^{57}$Co/Rh (activity $\cong$ 50 mCi) source and $\alpha$–Fe standard were used. The experimentally obtained spectra were fitted using CONFIT2000 software [14]. The parameters of hyperfine interaction such as isomer shift ($\delta$), quadrupole splitting ($\Delta$), effective internal magnetic field (B), line widths ($\Gamma_{exp}$), and relative weight (G) of the partial components in the spectra were determined.

**Table 3** Parameters of Mössbauer spectrum of $Cu_{0.5}Zn_{0.5}Fe_2O_4$ sample at LNT

| Sample | Components | $\delta$, mm/s | $\Delta$, mm/s | B, T | $\Gamma_{exp}$, mm/s | G, % |
|---|---|---|---|---|---|---|
| $Cu_{0.5}Zn_{0.5}Fe_2O_4$ | Sx1-tetra, A | 0.39 | 0.00 | 46.61 | 0.66 | 31 |
| | Sx2-octa, B1 (0.09) | 0.47 | 0.00 | 49.79 | 0.33 | 4 |
| | Sx3-octa, B2 (0.23) | 0.47 | 0.00 | 48.39 | 0.49 | 13 |
| | Sx4-octa, B3 (0.31) | 0.47 | 0.00 | 43.30 | 1.02 | 28 |
| | Sx5-octa, B4 (0.23) | 0.47 | 0.00 | 37.45 | 0.79 | 6 |
| | Sx6-octa, B5 (0.09) | 0.47 | 0.00 | 25.63 | 1.00 | 18 |

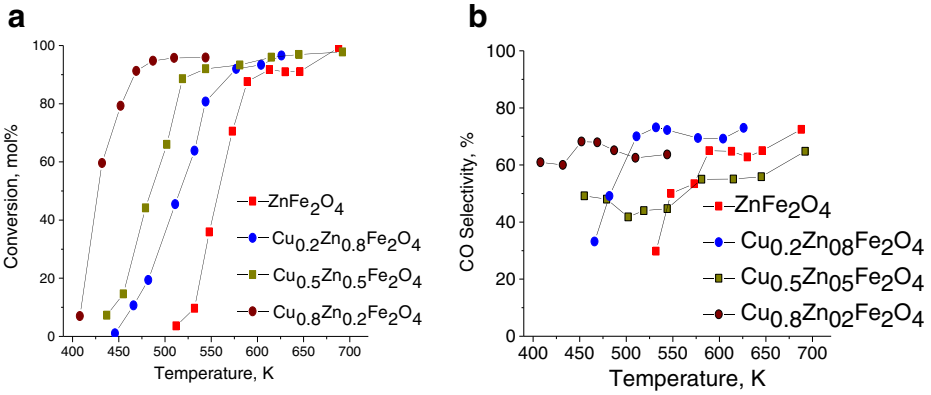


**Fig. 4** Methanol conversion (**a**) and CO selectivity (**b**) vs. temperature for various $Cu_{1-x}Zn_xFe_2O_4$ materials

### 2.3 Catalytic experiments

Methanol decomposition was carried out in a flow reactor at methanol partial pressure of 1.57 kPa and argon as a carrier gas (50 ml/min). The catalysts (0.055 g of catalyst) were tested under temperature-programmed regime within the range of 350–770 K and heating rate of 1 K/min. On-line gas chromatographic analyses were performed on a PLOT Q column using flame ionization and thermo-conductivity detectors. Absolute calibration method and a carbon based material balance were used for the calculation of conversion and the yields of the obtained products. The products selectivity was calculated as $Y_i/X*100$, where $Y_i$ is the current yield of the product i and X is methanol conversion.

## 3 Results and discussion

The XRD data for the obtained $Cu_{1-x}Zn_xFe_2O_4$ ferrites are presented in Fig. 1. All diffraction patterns revealed formation of well crystallized structure of cubic spinel phase at temperature used, which is in a good agreement with Thermogravimetry – Differential Thermal Analysis (TG-DTA) of hydroxide carbonate precursor of $Cu_{0.5}Zn_{0.5}Fe_2O_4$ presented in [15]. The endothermal effect in low temperature accompanied with a weight loss and exothermal effect without weight loss are established from TG-DTA analysis. The

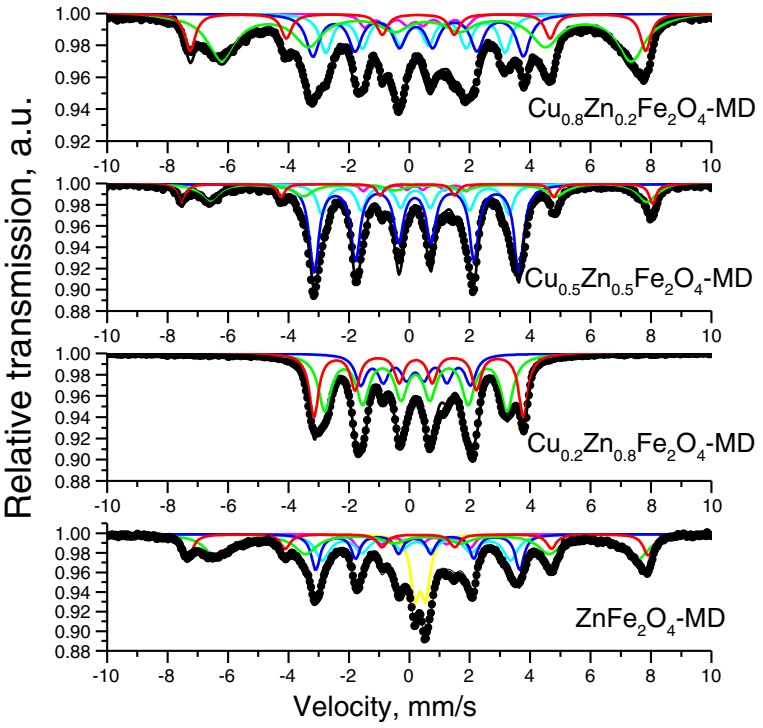


**Fig. 5** Mössbauer spectra of samples after catalytic test

endothermal effect could be assigned to dehydratation and decarbonisation of the hydroxide carbonate precursor. The appearance of exothermal effect with maximum at 795 K is referred to formation of Cu-Zn ferrite phase. The average crystallites size (D), degree of microstrain (e) and lattice parameters determined from XRD patterns are shown in Table 1. A well defined tendency for crystalline size increase from 19.08 nm to 24.39 nm with a simultaneous decrease of lattice constant in a range of 8.43-8.38 Å is observed for $Cu_{1-x}Zn_xFe_2O_4$ ferrites when x decreases from 1 to 0.2. The influence of crystalline size by chemical composition has been observed by other authors [16].

Room temperature Mössbauer spectra and parameters of hyperfine interactions as isomer shift, quadruple splitting and magnetic hyperfine field of the investigated samples are presented in Fig. 2 and Table 2, respectively. Mössbauer spectrum of pure $ZnFe_2O_4$ consists of doublet corresponding to paramagnetic behaviour of zinc ferrite where all amount of $Fe^{3+}$ions are located in B site of unit cell, while $Zn^{2+}$ ions strongly prefer A site position, determining zinc ferrite as a normal spinel. The Mössbauer parameters show no significant difference of magnetic structure when $x = 0.8$ and existence of paramagnetic phase was also observed. Mössbauer spectra exhibit sextet magnetic components with copper content increase in samples $Cu_{0.5}Zn_{0.5}Fe_2O_4$ and $Cu_{0.8}Zn_{0.2}Fe_2O_4$. In this case acceptable fitting of the experimental data could be obtained when the [B]-site pattern is assumed as superposition of more than one sextet. The binomial formula is used as a contrivance to calculated probability P(n, x) of an octahedral site having n nearest-neighbor zinc atoms in order to define the number of sextet components that have to use in the fitting model. Here the Mössbauer spectra are fitted with one sextet referred to tetrahedral coordination of $Fe^{3+}$

**Table 4** Parameters of Mössbauer spectra of $Cu_{1-x}Zn_xFe_2O_4$ after catalytic reaction of methanol decomposition

| Sample | Components | $\delta$, mm/s | $\Delta$, mm/s | B, T | $\Gamma_{exp}$, mm/s | G, % |
|---|---|---|---|---|---|---|
| $ZnFe_2O_4$-MD | M-Sx1, $Fe_{3-x}Me_xO_4$ | 0.30 | – | 47.2 | 0.39 | 12 |
| | M-Sx2, $Fe_{3-x}Me_xO_4$ | 0.59 | – | 43.2 | 0.88 | 30 |
| | C-Sx1, $\chi$-$Fe_5C_2$ | 0.30 | 0.10 | 21.0 | 0.36 | 18 |
| | C-Sx2, $\chi$-$Fe_5C_2$ | 0.23 | 0.00 | 19.3 | 0.57 | 20 |
| | C-Sx3, $\chi$-$Fe_5C_2$ | 0.17 | 0.02 | 11.5 | 0.38 | 7 |
| | Db, $ZnFe_2O_4$ | 0.36 | 0.35 | – | – | 13 |
| $Cu_{0.2}Zn_{0.8}$ $Fe_2O_4$-MD | C-Sx1, $\chi$-$Fe_5C_2$ | 0.26 | 0.10 | 21.5 | 0.37 | 31 |
| | C-Sx2, $\chi$-$Fe_5C_2$ | 0.21 | 0.01 | 18.73 | 0.51 | 47 |
| | C-Sx3, $\chi$-$Fe_5C_2$ | 0.20 | 0.01 | 11.3 | 0.43 | 22 |
| $Cu_{0.5}Zn_{0.5}$ $Fe_2O_4$-MD | M-Sx1, $Fe_{3-x}Me_xO_4$ | 0.26 | −0.00 | 48.4 | 0.28 | 8 |
| | M-Sx2, $Fe_{3-x}Me_xO_4$ | 0.66 | −0.03 | 44.8 | 0.75 | 17 |
| | C-Sx1, $\chi$-$Fe_5C_2$ | 0.21 | 0.05 | 21.0 | 0.37 | 52 |
| | C-Sx2, $\chi$-$Fe_5C_2$ | 0.20 | −0.00 | 19.0 | 0.38 | 19 |
| | C-Sx3, $\chi$-$Fe_5C_2$ | 0.18 | 0.00 | 10.0 | 0.27 | 3 |
| $Cu_{0.8}Zn_{0.2}$ $Fe_2O_4$-MD | M-Sx1, $Fe_{3-x}Me_xO_4$ | 0.29 | −0.01 | 46.8 | 0.42 | 14 |
| | M-Sx2, $Fe_{3-x}Me_xO_4$ | 0.57 | −0.01 | 42.0 | 1.11 | 40 |
| | C-Sx1, $\chi$-$Fe_5C_2$ | 0.25 | 0.06 | 21.6 | 0.52 | 22 |
| | C-Sx2, $\chi$-$Fe_5C_2$ | 0.18 | 0.03 | 18.4 | 0.48 | 19 |
| | C-Sx3, $\chi$-$Fe_5C_2$ | 0.19 | 0.01 | 10.4 | 0.41 | 5 |

ions [A]-site and five sextets for x = 0.5 and four sextet for x = 0.2 with parameters of $Fe^{3+}$ ions in octahedral position [B]-site of unit cell. The existence of number of sextet components with different hyperfine field can be explained with random occupancy of tetrahedral positions of spinel lattice by $Fe^{3+}$ and diamagnetic $Zn^{2+}$ions, which results in existence of different (A) site nearest neighbors of [B]-site $Fe^{3+}$i.e. 6Fe, 5Fe and 1Zn, 4Fe and 2Zn and etc. (A)-site neighbors (corresponding sextet components are shown in Table 2, as B0, B1, B2 and etc., followed by calculated probability in parenthesis).

Mössbauer spectrum of sample $Cu_{0.5}Zn_{0.5}Fe_2O_4$ was collected in temperature of liquid nitrogen and the parameters of hyperfine interaction were estimated (Fig. 3 and Table 3). In low temperature spectrum, there is no effect of relaxation and well defined sextet components have been observed.

Temperature dependencies of methanol conversion and CO selectivity for all ferrite materials are presented in Fig. 4. The obtained ferrites range in the order of increase of catalytic activity according to the increase of copper content in them. The sample $Cu_{0.8}Zn_{0.2}Fe_2O_4$ demonstrates extremely high catalytic activity and 90 % conversion is achieved at about 460 K. The selectivity to CO for all materials is between 40 and 70 % and above 500 K it is slightly higher for the sample with the lowest copper content ($Cu_{0.2}Zn_{0.8}Fe_2O_4$). The main registered by-product during the decomposition is $CO_2$ (up to 30–40 %) and $CH_4$(up to 5–10 %).

The Mössbauer spectroscopy analyses of the samples after catalytic test demonstrate significant reduction transformations with the ferrites under the reaction medium (Fig. 5 and Table 4). The calculated Mössbauer parameters reveal presence of magnetite phase ($Fe_3O_4$) that consist of two sextets which are referred to $Fe^{3+}$ in tetra- and $Fe^{2.5+}$ in octa- positions,

denoted in Table 4 as M-Sx1 and M-Sx2, respectively. However their relative weight ratio is smaller than 1 : 1.88, which is typical for the pure stoichiometric $Fe_3O_4$phase. Thus, we assume that the Fe ions in magnetite are partially substituted by $Me^{2+}$ (Me = Zn, Cu) i.e. it is formed Me-substituted magnetite with general formula $Fe_{3-x}Me_xO_4$. The formation of Me-substituted magnetite and carbide of Hägg ($\chi$-$Fe_5C_2$) in different proportion have been detected for all catalysts, except $Cu_{0.2}Zn_{0.8}Fe_2O_4$, in which only $\chi$-$Fe_5C_2$ phase is observed. The relative part of the Me-substituted magnetite increases with the increase of copper content in ferrites and only in the case of $ZnFe_2O_4$ presence of non-changed zinc ferrite phase with G = 13 % is observed. We consider that the catalytic activity of ferrites increases with the increase of copper content in them and well correlates with their further transformation to Me-substituted magnetite. It is not excluded the extremely high catalytic activity of the samples with high copper content to be related to the decomposition of ferrite under the reaction medium with the formation of finely dispersed copper nanoparticles in close contact with Me-substituted magnetite which in a synergistic activity promotes the decomposition of methanol and the release of hydrogen from the catalyst surface.

## 4 Conclusion

Nanodimentional $Cu_{1-x}Zn_xFe_2O_4$ ferrites with different composition were synthesised using co-precipitation and thermal methods. A well defined tendency for the ferrite crystallite size increase with the copper content increase is registered. The ferrite materials exhibit high catalytic activity in methanol decomposition which increases with the increase of copper content in the samples. The catalytic behaviour of ferrites in methanol decomposition strongly depends on the phase transformations that occur by the influence of the reaction medium.

**Acknowledgments** The authors express their gratitude for the financial support by Bulgarian National Science Fund (NSF) under Project NSF-E01/7/2012 for carrying out the research work on the program. K. K. and N. V. acknowledge sponsorship by European Social Fund (ESF) under the Operating Program "Development of Human Resources" Project BG051PO001-3.3.06-0050 enabling for their participation in ICAME-2013 and the presentation of the experimental results.

## References

1. Nowika, I., Felnera, I., Garcia-Miquela, H.: Mössbauer spectroscopy studies of spin reorientations in amorphous and crystalline $(Co_{0.2}Fe_{0.8})_{72.5}Si_{12.5}B_{15}$ glass coated micro-wires. J. Magn. Magn. Mater **311**, 555–559 (2007)
2. Schrödera, C., Bailey, B., Klingelhöfer, G., Staudigel, H.: Fe Mössbauer spectroscopy as a tool in astrobiology. Planet. Space Sci. **54**, 1622–1634 (2006)
3. Oshtrakh, M.I., Grokhovsky, V.I., Petrova, E.V., Larionov, Y.M., Goryunov, M.V., Semionkin, V.A.: Mössbauer spectroscopy with a high velocity resolution applied for the study of meteoritic iron-bearing minerals. J. Mol. Struct. **1044**, 268–278 (2013)
4. Oshtrakha, M.I., Semionkina, V.A.: Mössbauer spectroscopy with a high velocity resolution: advances in biomedical, pharmaceutical, cosmochemical and nanotechnological research. Spectrochim. Acta A **100**, 78–87 (2013)
5. Oshtrakh, M.I., Alenkina, I.V., Milder, O.B., Semionkin, V.A.: Mössbauer spectroscopy with a high velocity resolution in the study of iron-containing proteins and model compounds. Spectrochim. Acta A **79**, 777–783 (2011)

6. Mittal, V.K., Chandramohan, P., Bera, S., Srinivasan, M.P., Velmurugan, S., Narasimhan, S.V.: Cation distribution in $Ni_xMg_{1-x}Fe_2O_4$ studied by XPS and Mössbauer spectroscopy. Solid State Commun. **137**(1–2), 6–10 (2006)
7. Manova, E., Paneva, D., Kunev, B., Estournès, C., Rivière, E., Tenchev, K., Léaustic, A., Mitov, I.: Mechanochemical synthesis and characterization of nanodimensional iron–cobalt spinel oxides. J. Alloy. Comp. **485**, 356–361 (2009)
8. Manova, E., Tsoncheva, T., Paneva, D., Mitov, I., Tenchev, K., Petrov, L.: Mechanochemically synthesized nano-dimensional iron–cobalt spinel oxides as catalysts for methanol decomposition. Appl. Catal. A Gen. **277**, 119–127 (2004)
9. Manova, E., Tsoncheva, T., Paneva, D., Popova, M., Velinov, N., Kunev, B., Tenchev, K., Mitov, I.: Nanosized copper ferrite materials: mechanochemical synthesis and characterization. J. Solid State Chem. **184**, 1153–1158 (2011)
10. Velinov, N., Koleva, K., Tsoncheva, T., Manova, E., Paneva, D., Tenchev, K., Kunev, B., Mitov, I.: Nanosized $Cu_{0.5}Co_{0.5}Fe_2O_4$ ferrite as catalyst for methanol decomposition: effect of preparation procedure. Catal. Commun. **32**, 41–46 (2013)
11. Millet, J.-M.M.: Mössbauer spectroscopy in heterogeneous catalysis. Adv. Catal. **51**, 309–350 (2007)
12. Velinov, N., Manova, E., Tsoncheva, T., Estournes, C., Paneva, D., Tenchev, K., Petkova, V., Koleva, K., Kunev, B., Mitov, I.: Solid State Sci. **14**, 1092 (2012)
13. Kraus, W., Nolze, G.: PowderCell for Windows. Federal Institute for Materials Research and Testing, Berlin (2000)
14. Žák, T., Jirásková, Y.: CONFIT: Mössbauer spectra fitting program. Surf. Int. Anal. **38**(4), 710–714 (2006)
15. Koleva, K.V., Velinov, N.I., Tsoncheva, T.S., Petkova, V.S., Shopska, M.G., Mitov, I.G.: Synthesis and catalytic properties of $Cu_{0.5}Zn_{0.5}Fe_2O_4$ ferrite. Int. Sci. Publ. Mater. Method Technol. **7**(1), 362–371 (2013)
16. Rana, M.U., Misbah-ul, I., Abbas, T.: Cation distribution and magnetic interactions in Zn-substituted $CuFe_2O_4$ ferrites. Mater. Chem. Phys. **65**, 345–349 (2000)